**Proceedings of the ASME 2020 15th International Manufacturing Science and Engineering Conference
MSEC2020
September 3, 2020, Virtual, Online**

MSEC2020-8377

DUAL EXTRUSION FDM PRINTER FOR FLEXIBLE AND RIGID POLYMERS

Garrett McGrady
University of Louisville
Louisville, KY

Kevin Walsh
University of Louisville
Louisville, KY

ABSTRACT

Commercially available fused deposition modeling (FDM) printers have yet to bridge the gap between printing soft, flexible materials and printing hard, rigid materials. This work presents a custom printer solution, based on open-source hardware and software, which allows a user to print both flexible and rigid polymer materials. The materials printed include NinjaFlex, SemiFlex, acrylonitrile-butadiene-styrene (ABS), Nylon, and Polycarbonate.

In order to print rigid materials, a custom, high-temperature heated bed was designed to act as a print stage. Additionally, high temperature extruders were included in the design to accommodate the printing requirements of both flexible and rigid filaments. Across 25 equally spaced points on the print plate, the maximum temperature difference between any two points on the heated bed was found to be ~9°C for a target temperature of 170°C. With a uniform temperature profile across the plate, functional prints were achieved in each material.

The print quality varied, dependent on material; however, the standard deviation of layer thicknesses and size measurements of the parts were comparable to those produced on a Zortrax M200 printer. After calibration and further process development, the custom printer will be integrated into the NEXUS system—a multiscale additive manufacturing instrument with integrated 3D printing and robotic assembly (NSF Award #1828355).

1. INTRODUCTION

In rapid prototyping, fused deposition modeling is a 3D printing method by which layers of material are printed successively, bottom to top [1]. FDM is often used to print static prototypes, and it is widely used in research laboratory settings to print parts on-demand [2]. There are many materials on the market that are available as filaments, including both flexible and rigid polymer materials. However, there are no commercially available, open-source printers that can print a large range of both soft and rigid filaments. The lack of such a printer is largely driven by the higher temperature requirements for printing rigid materials such as polycarbonate.

In addition to varying bed and extruder temperature requirements, the extrusion of soft and rigid materials can be challenging because soft materials are more likely to build up and clog the system between the extrusion wheel and the heater block. Thus, the extrusion speed and optimal tension between extruder gear and filament changes for different materials.

This research seeks to develop a custom printer solution, which can print both soft and rigid polymers, using a dual-extruder setup. To minimize cost, the printer was designed using open-source hardware and software. Eventually, the printer will be incorporated into the NEXUS system—a multiscale additive manufacturing instrument with integrated 3D printing and robotic assembly (NSF Award #1828355). Designing a custom, open-source FDM printer such as the one presented here allows for easier integration into the NEXUS system later, where the dual extrusion system will function as a toolhead on a robotic manipulator.

2. MATERIALS AND METHODS

2.1 Printer System Architecture

A low-cost solution to multi-material printing requires the use of open-source software and hardware. The control software used on the machine was Octoprint, and a Smoothieboard X5 V1.1 was used as an open-source hardware solution to control the FDM printer hardware.

Octoprint was hosted on a Raspberry Pi 3 Model B+. A monitor was connected to the Raspberry Pi to obtain the IP address of the Octoprint instance, allowing the team to control the printer from the browser of a laptop. Commands were sent from the browser over a local-area-network, where they are received on the Pi and communicated to a controller card via USB connection.

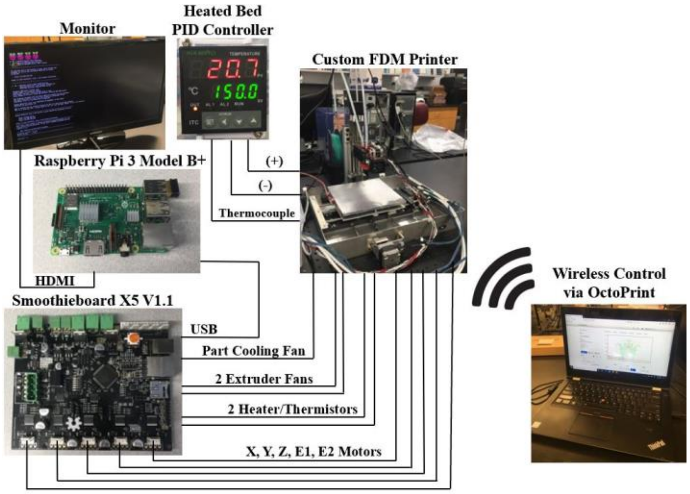

FIGURE 1: SCHEMATIC DIAGRAM OF FDM SYSTEM

The Smoothieboard X5 V1.1 controller card accommodates five axes. As Figure 1 shows, the heated bed was controlled with a PID controller, on its own dedicated circuit.

2.2 Heated Bed Design

Since the printer was meant to print a variety of flexible and rigid polymers, the design specification required a heated bed that could provide both low (100-130ºC) and high (140-170ºC) temperatures for flexible and rigid materials, respectively. The agreed design specification was that the heated bed be capable of 170ºC, implement a three-point leveling system, and accommodate in-situ part processing. A 420W, 6"x7" silicone rubber heater was placed underneath a 1/4" aluminum spreader plate, which sat under a 1/8" aluminum print plate [3]. Using a silicone heater with a specified power density of $10W/in^2$ ensured that the time to heat would be reasonable for temperatures of 100 to 170ºC. Additionally, using a spreader plate ensured a uniform distribution of thermal energy beneath the print plate. The print plate is held in place on the spreader plate by two keyed guide pins, allowing it to be easily removed in the case of in-situ part processing.

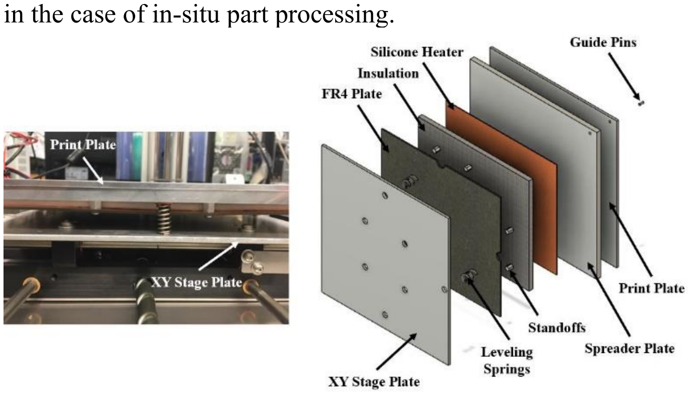

FIGURE 2: (LEFT) FRONT VIEW OF HEATED BED ASSEMBLY, (RIGHT) EXPLODED VIEW OF HEATED BED COMPONENTS

The silicone heater was surrounded by spacers, which held its XY position on the spreader plate while also bracing a piece of aerogel insulation between the heater and a plate of FR4. Finally, springs were used between the spreader plate and an XY stage plate to implement a manual, three-point leveling system.

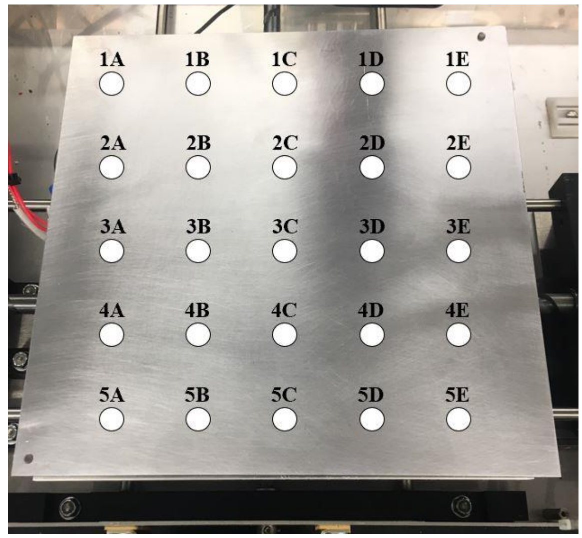

FIGURE 3: REGION/POINT INDEXING FOR HEATED BED

To quantify the uniformity of print plate temperature, thermal grease was placed in 25 equally spaced points across the plate. Then, once the PID controller had reached a target temperature, readings were recorded at each point using a thermocouple and multimeter. It is important to note that the PID controller's feedback measurement is from a K-Type thermocouple, which is mounted near region 3A, under the spreader plate.

2.3 Dual Extruder Setup

Extruding both flexible and rigid polymers presents a challenge since, typically, more rigid polymers require a much higher temperature to change phase. Additionally, the extrusion of soft, flexible materials often fails when filament is not properly guided into the heater block. Anticipating these issues, the team chose to implement a Flexion high-temperature, dual extruder system. This extruder package, from Diabase, includes low temperature and high temperature printhead assemblies (see Figure 4). Each printhead was outfitted with 0.4mm nozzles.

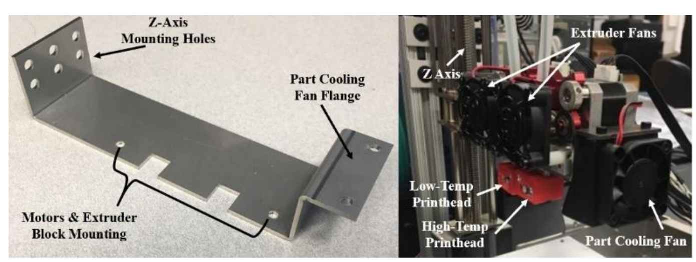

FIGURE 4: (LEFT) DUAL EXTRUDER MOUNTING BRACKET, (RIGHT) FULLY ASSEMBLED PRINTHEAD AND EXTRUDER SYSTEM, MOUNTED ON Z-AXIS

A custom bracket was designed and fabricated to hold the extruder system, extruder stepper motors, printheads, and cooling fans during print. The bracket was then mounted on a z-axis, which was stationary beside the print stage's XY gantry. Due to the fixed XY position of the printhead and the size of the heated bed, the printer had capability to print an XY area of 65x65mm.

2.4 Printable Materials

The objective of designing a custom printer was to allow for printing of both flexible and rigid polymer materials. In order of shore's hardness, from soft to hard, the materials selected were NinjaFlex, SemiFlex, ABS, Nylon, and Polycarbonate [5-7]. Table 1 shows the print recipe for each material, which was optimized experimentally in a pilot study [8-11]. The print speed for all recipes was 30mm/s.

TABLE 1: PRINT RECIPES BY MATERIAL

Material	Extruder Temp. (ºC)	Bed Temp. (ºC)	Shore Scale	Part Cooling (Y/N)	Adhesion Method
NinjaFlex	255	130	85A	Y	None
SemiFlex	235	110	98A	Y	None
ABS	265	130	76D	Y	Brim
Nylon	275	140	80D	N	Brim
Polycarbonate	290	150	86D	N	Brim

In pilot experiments, it was found that using a higher bed temperature promoted that adhesion of plastics on the aluminum print plate. The bed temperature reported in Table 1 is the temperature being read at the bottom of the spreader plate; therefore, it is higher than the operating temperature at the top of the print plate (see Section 3.1). In addition to using high bed temperatures, for some materials, a brim adhesion method was used. The brim is a skirt of material that surrounds the first layer of a printed part, reducing the probability for part warping.

2.5 Filament Storage

A common print quality issue, especially with rigid polymers such as polycarbonate and nylon, is the absorption of moisture in air over time. Filaments that are allowed to absorb moisture will result in a poor surface quality and rough, non-uniform layers.

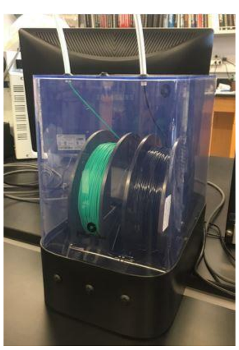

FIGURE 5: AIRTIGHT FILAMENT STORAGE REDUCES MOISTURE ABSORPTION OF NINJAFLEX (GREEN) AND POLYCARBONATE (BLACK)

To mitigate this issue, filaments were stored in an airtight container with desiccant packages (see Figure 5). The humidity within the container was maintained at ~10%. Prior to placing filaments in the container for storage and/or printing, they were baked in an oven at 80ºC for 24hrs.

3 RESULTS AND DISCUSSION

3.1 Temperature Uniformity of Heated Bed

In 25 equally space points across the 8"x8" heated bed, a print plate temperature was recorded to ensure adequate uniform heating (see Figure 6). The differential temperature is the difference between print plate temperature and the temperature recorded by the PID controller (see Heated Bed Design).

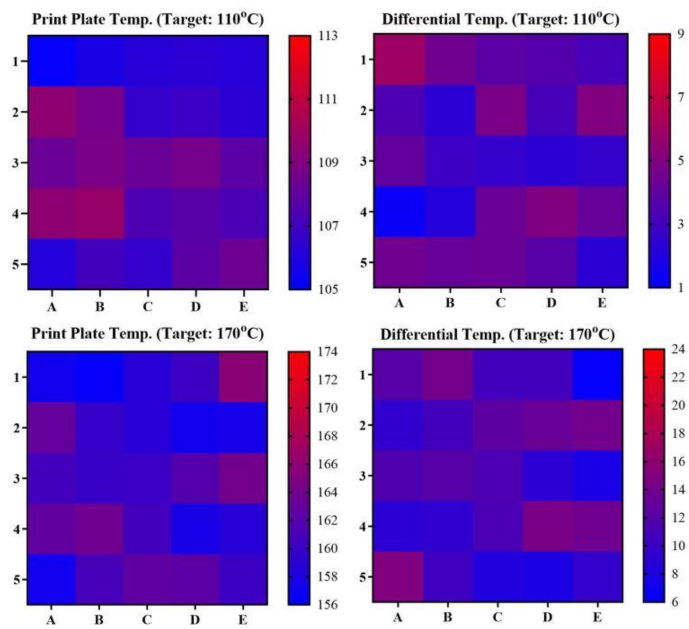

FIGURE 6: PRINT PLATE AND DIFFERENTIAL TEMPERATURES FOR TARGETS OF 110ºC AND 170ºC.

For a PID target temperature of 110ºC, the average print plate temperature was 107.5ºC, with a standard deviation of 1.2ºC. The range of print plate temperatures for a 110ºC target was 4.6ºC, and the average differential between print plate temperature and the PID reading was 3.6ºC.

For a PID target temperature of 170ºC, the average print plate temperature was 160.3ºC, with a standard deviation of 2.5ºC. The range of print plate temperatures for a 170ºC target was 9.4ºC, and the average differential between print plate temperature and the PID reading was 11.0ºC.

As target temperature increases, the difference between print plate temperature and the PID reading increases. Additionally, the range and deviation of print plate temperatures increases with a higher target temperature. However, the observed temperature deviations across the 25 points are not large enough to significantly affect part adhesion while printing.

In the future, the PID controller target temperature can be calibrated to ensure that print plate temperature is reaching the target temperature.

3.2 Printed Part Quality

Print quality was assessed by measuring average layer thickness *t*, part length *L*, part width *W*, and part height *H* [8]. The target geometry for test specimens was $L = 40$mm, $W = 10$mm, $H = 5$mm, and target *t* was varied according to each material's optimized print recipe. Figure 7a-7f shows the side view of each material, and Figure 7g shows the top view of each material. In Figure 7f, for polycarbonate, there appear to be irregularities in the layer quality, which is likely a symptom of the filament not being completely dehydrated during printing (see Filament Storage).

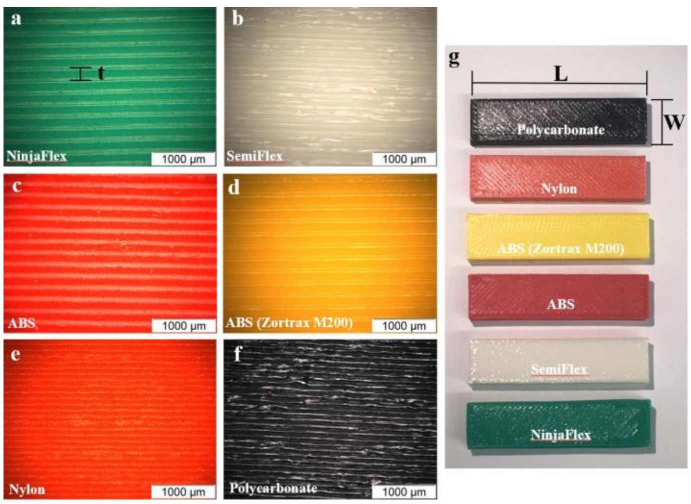

FIGURE 7: PRINTED MATERIALS FROM CUSTOM PRINTER

As a basis for comparison, a proprietary Zortrax ABS filament was printed on a Zortrax M200 machine. Table 2 shows the resulting measurements of each material, including the results of the Zortrax M200 printer. According to the lower-than-expected average values of *L* and *W* for each material, the number of steps per mm of the custom printer in the X and Y directions may need to be adjusted within the firmware for future prints. The SemiFlex layer thickness was not observable with a light microscope, but the standard deviation of layer thicknesses within the other materials are comparable to the deviation observed in the Zortrax M200 part. Finally, the value of *H* for the custom printer is dependent on the print material, where some materials undershoot, and others overshoot the target of 5mm.

TABLE 2: PRINT DIMENSIONS AND STD. DEVIATIONS

Material	Target *t* (um)	Actual *t* (um)	*L* (mm)	*W* (mm)	*H* (mm)
NinjaFlex	200	195 (± 9)	39.77 (± 0.05)	10.12 (± 0.04)	5.17 (± 0.04)
SemiFlex	100	94 (±8)	39.01 (± 0.11)	9.72 (± 0.04)	5.02 (± 0.03)
ABS	200	187 (± 12)	39.26 (± 0.09)	9.80 (± 0.02)	5.36 (± 0.04)
Nylon	100	97 (± 9)	39.05 (± 0.02)	9.84 (± 0.02)	4.99 (± 0.03)
Polycarb.	100	95 (± 8)	39.17 (± 0.06)	9.66 (± 0.02)	5.15 (± 0.04)
ABS (Zortrax M200)	190	206 (± 13)	40.00 (± 0.05)	10.06 (± 0.05)	5.09 (± 0.01)

3.3 Concurrent Printing

In addition to printing one flexible or rigid polymer in each print run, the team also attempted to dual-extrude materials of different hardness concurrently. NinjaFlex and Polycarbonate materials were printed side-by-side, where the temperature of the heated bed was chosen to remain at Polycarbonate's heated bed temperature of 150ºC. Choosing the high temperature as a common value for both materials resulted in print quality inconsistencies in the NinjaFlex material. Further experiments need to be carried out to develop an appropriate process flow for dual extrusion slicing and printing. In the future NEXUS system, the issues of concurrent printing may be resolved by investigating how to print these materials by independently actuating each printhead when it is active. Independent actuation of each extruder would also give spatial clearance when operating this dual extrusion system on the end of a 6-axis robotic arm [12-13].

4 CONCLUSION

The custom heated bed and extruder assembly presented here allow for printing both soft and rigid substrates. The printable material extremes of this system are NinjaFlex and Polycarbonate, which have a shore scale hardness of 85A and 86D, respectively. The capability to print this range of materials was largely due to the heated bed, which exhibited uniform temperature across the print plate at a target temperature of 170ºC and accommodated a removable print plate for the option of in-situ part processing.

The goal of this work was to develop an open-source FDM solution for printing both flexible and rigid polymers, and it has been successfully demonstrated. While concurrent printing of different materials requires additional process development, the machine presented here is able to print each material with similar geometric consistency as a commercially available Zortrax M200. When the FDM printer is integrated into the NEXUS system as a toolhead on a robotic manipulator, users will have the capability to embed electronics in both flexible and rigid substrates.

ACKNOWLEDGEMENTS
This research was supported by National Science Foundation Award #1828355, which is part of a Major Research Instrumentation. The work has also been supported, in part, by National Science Foundation Award ECCS-1542164, which is part of the NSF National Nanotechnology Coordinated Infrastructure (NNCI).

REFERENCES
[1] Ivan Gajdoš, Jan Slota, "Influence of Printing Conditions on Structure in FDM Prototypes," *Technical Gazette* 20, no. 2 (2013).
[2] Meghan Coakley, Darrell Hurt, "3D Printing in the Laboratory: Maximize Time and Funds with Customized and Open-Source Labware," *Journal of Laboratory Automation* 21, no. 4 (2016), doi:10.1177/2211068216649578
[3] Diana Popescu, et al., "FDM process parameters influence over the mechanical properties of polymer specimens: A review," *Polymer Testing* 69, (2018), https://doi.org/10.1016/j.polymertesting.2018.05.020
[4] *Flexible Silicone Rubber Fiberglass Insulated Heaters*, Omega.
[5] *NinjaFlex 3D Printing Filaments Technical Specifications*, NinjaTek.
[6] Wei Dai Vian, Nancy Denton, "Hardness Comparison of Polymer Specimens Produced with Different Processes," ASEE IL-IN Section Conference 3, (2018).
[7] *Shore Scale*, 3D Systems Learning Center, https://www.3dsystems.com/quickparts/learning-center/shore-scale
[8] Stefano Moscato, et al., "Infill-Dependent 3-D-Printed Material Based on NinjaFlex Filament for Antenna Applications," *IEEE Antennas and Wireless Propagation Letters* 15, (2016)
[9] F. Knoop, V. Schoeppner, "Mechanical and Thermal Properties of FDM Parts Manufactured with Polyamide 12," University of Paderborn.
[10] Miquel Domingo-Espin, et al., "Mechanical property characterization and simulation of fused deposition modeling Polycarbonate parts," *Materials & Design* 83, (2015), http://dx.doi.org/10.1016/j.matdes.2015.06.074
[11] Evgeniy Gordeev, et al., "Improvement of quality of 3D printed objects by elimination of microscopic structural defects in fused deposition modeling," *PLoS One* 13, no. 6 (June 2018), https://doi.org/10.1371/journal. pone.0198370
[12] Yeo Jung Yoon, et al., "Development of Three-Nozzle Extrusion System for Conformal Multi-Resolution 3D Printing with a Robotic Manipulator," *ASME IDETC/DIE*, DETC2019-98069, (2019).
[13] Prahar Bhatt, et al., "A Robotic Cell for Multi-Resolution Additive Manufacturing," *2019 International Conference on Robotics and Automation (ICRA)*, Montreal, QC, Canada, 2019, pp. 2800-2807.